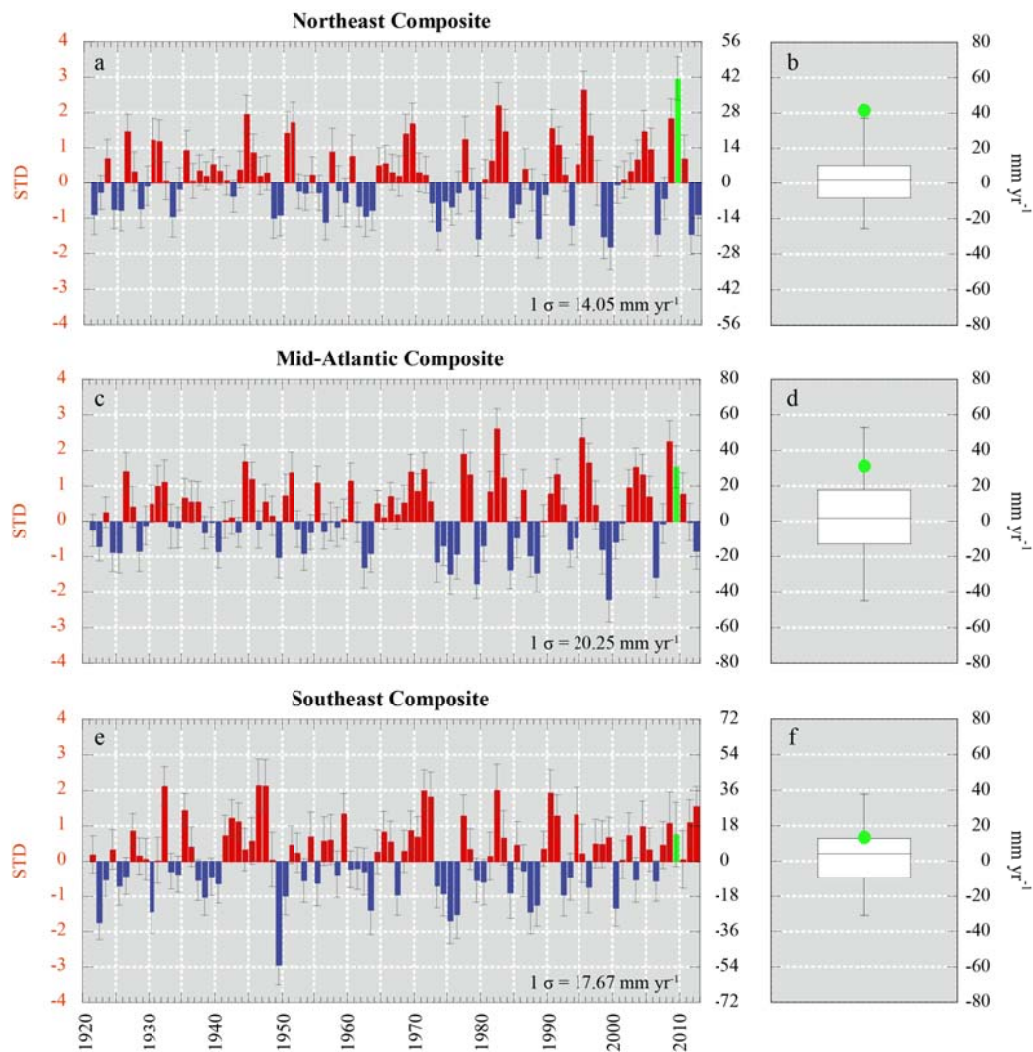**Supplementary Figure 1. Total coastal SLR over 2008-2010 from TG stations.** The separation at New York City is evident. The sea level jump is large (relatively small) north (south) of New York City.

Supplementary Figure 2. Yearly SLR rate based on linear fits to the monthly data on interannual time scale (36 months). **a., c. and e**. Time series of the yearly SLR rates (mm yr^{-1}). The absolute and relative (to 1σ) rates are shown by the right and left y-axis, respectively. The rate is centered about the year of interest. Rates are calculated only if all 36-month data are available. **b., d. and f.** Box and whisker plots indicate the position of the 2009 SLR rate for the Northeast, Mid-Atlantic and Southeast SLR regions. The 2009 SLR rates are depicted by green bars and dots.
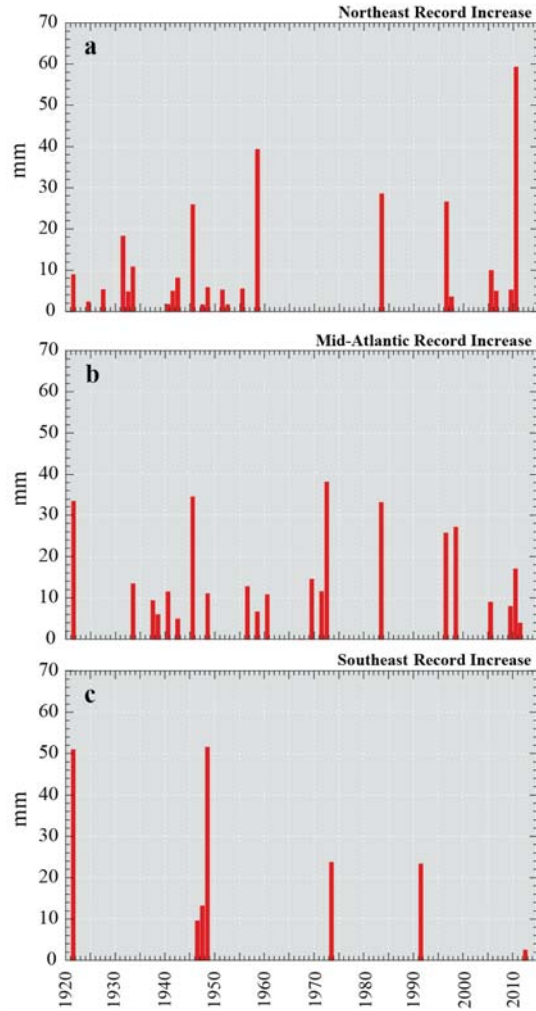
Supplementary Figure 3. Years with record high sea levels in the three SLR regimes. The values show the sea level increase over the previous record sea level (mm).
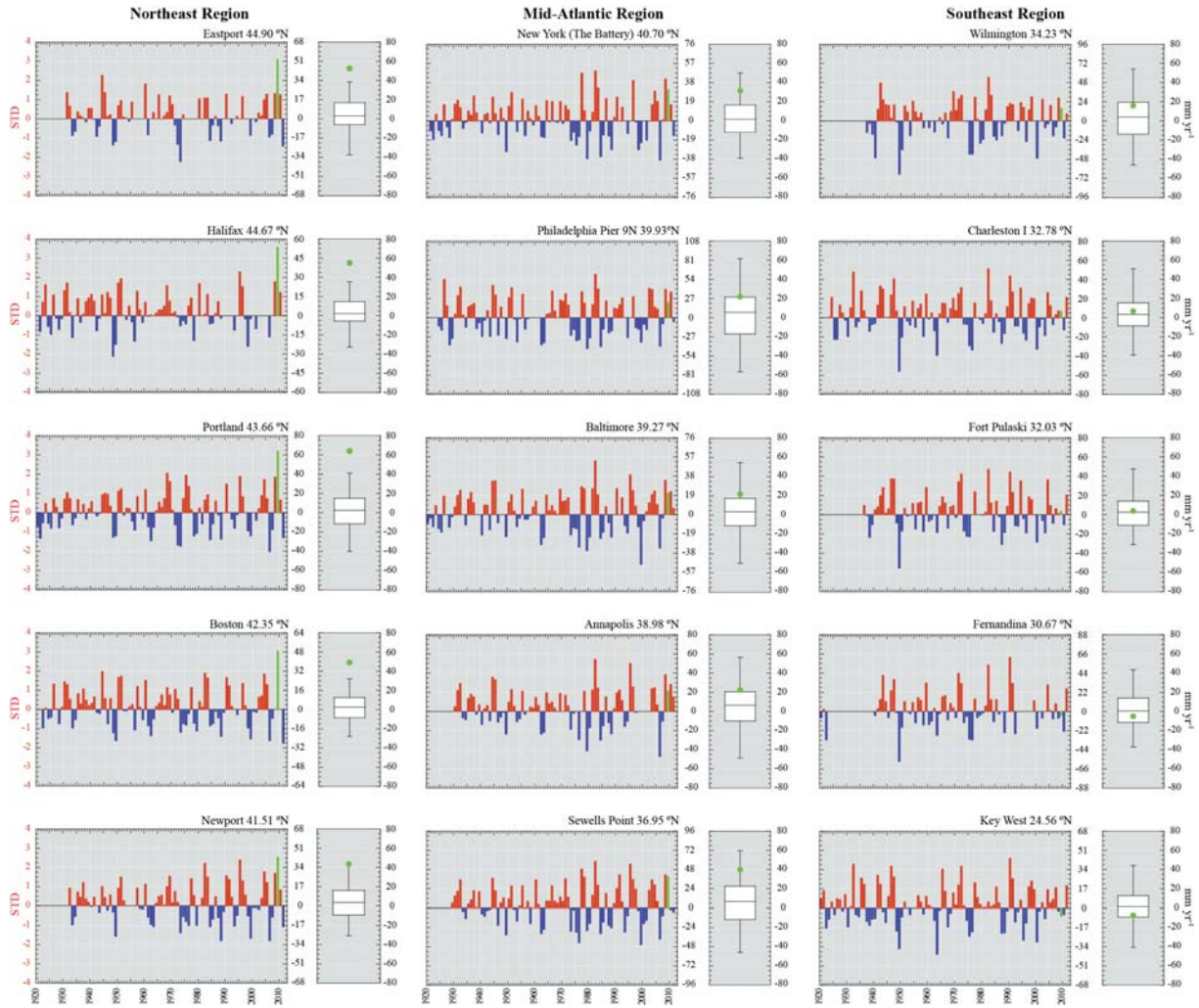
Supplementary Figure 4. Individual TG station records from the three SLR regimes. The left, middle and right columns contains records for TG stations locations in the Northeast, Mid-Atlantic and Southeast regions, respectively. The absolute and relative (to 1σ) rates are shown by the right and left y-axis, respectively. Each box plot represents the median, upper and low quartile, minimum and maximum values that fall within an acceptable range given a TG record, and outliers that do not fall within this acceptable range. Specifically, an outlier is a point whose value is greater (less) than the upper (lower) quartile plus (minus) 1.5 times the interquartile distance (the distance between the upper and lower quartiles). The 2009 data are depicted by green bars and dots.

4
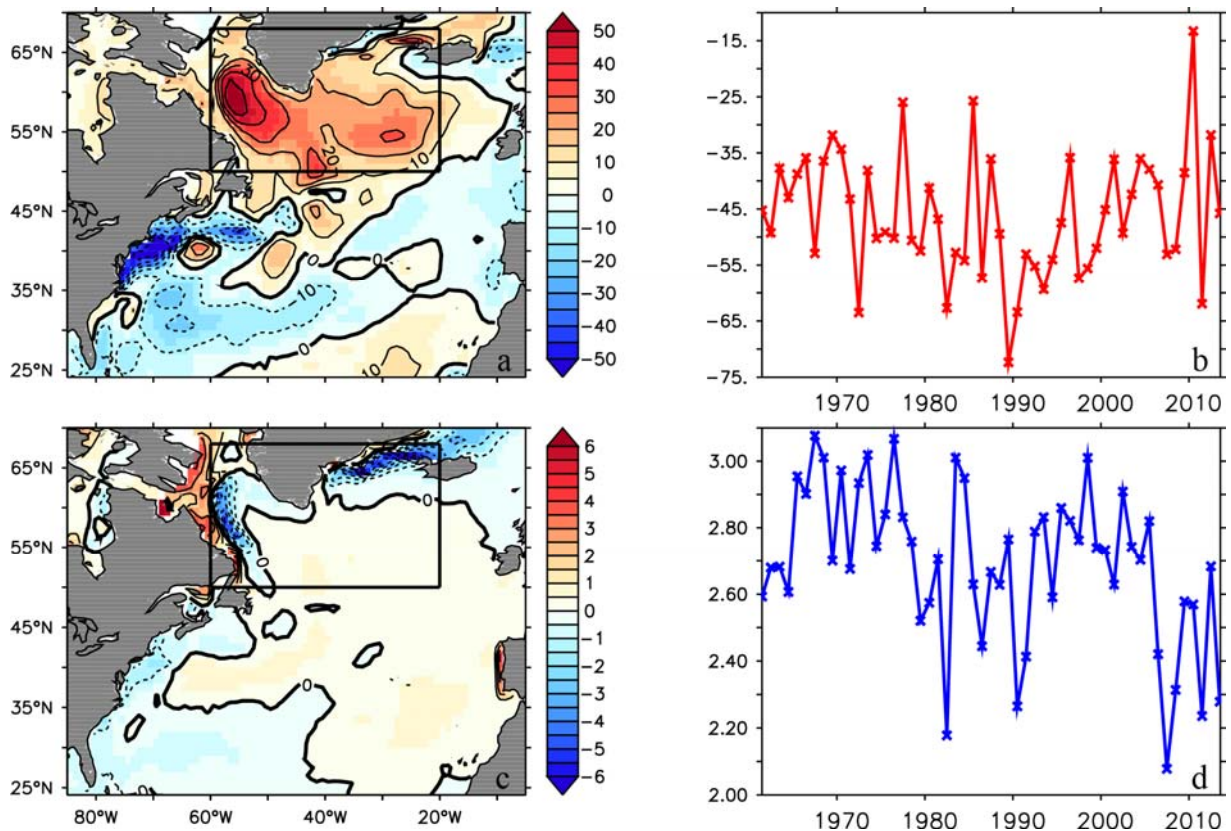
Supplementary Figure 5. Heat and freshwater flux anomalies in 2009-10 relative to 1961-2013. a. Heat flux anomalies (contour interval - 10 W m^{-2}). **b.** Time series of the mean heat flux within the black box from 1961 – 2013 (W m^{-2}). **c.** Freshwater flux anomalies (contour interval - 2x10^8 m s^{-1}). **d.** Time series of the mean freshwater flux within the black box (10^8 m s^{-1}). The data are from the GFDL ODA.
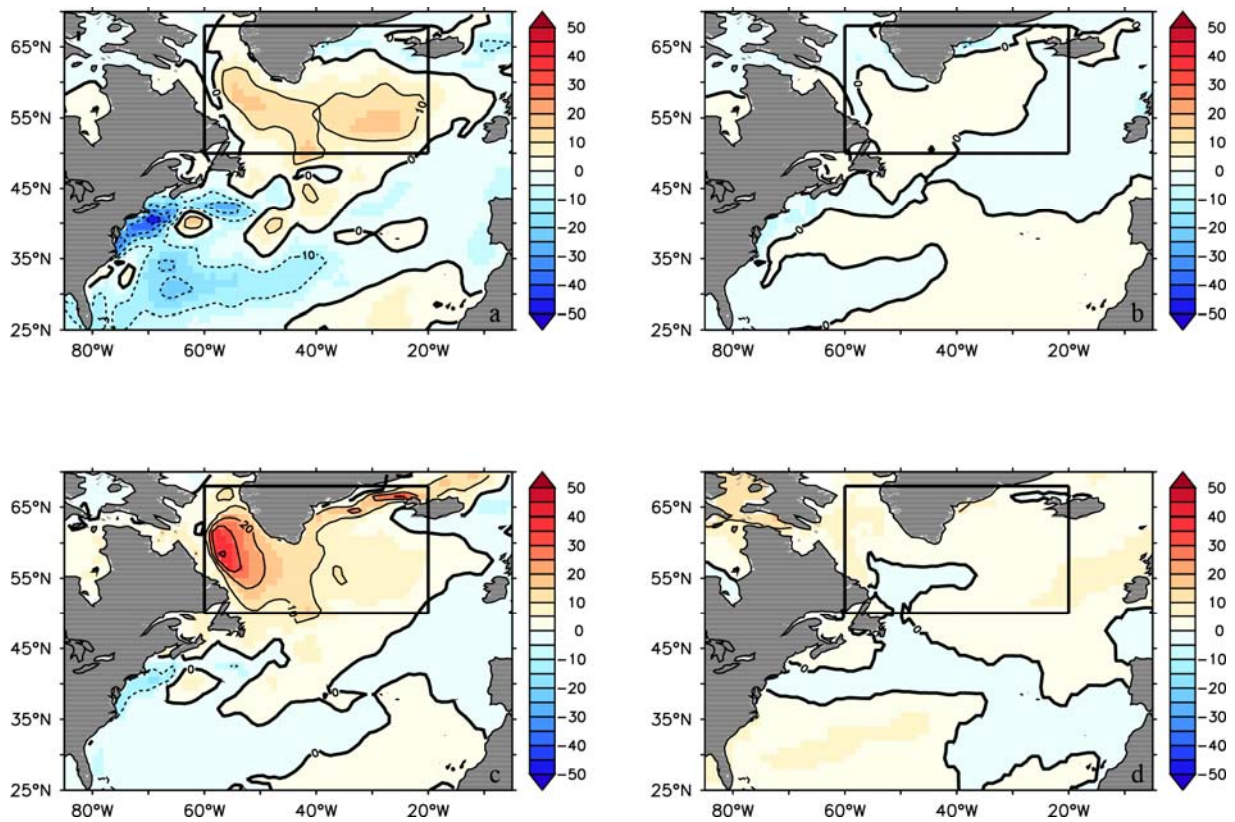
Supplementary Figure 6. Components of the heat flux anomalies (W m^{-2}) in 2009-10 relative to 1961 – 2013. a. Latent heat flux anomaly into the ocean (contour interval - 10 W m^{-2}). **b.** Longwave heat flux anomaly into the ocean. **c.** Sensible heat flux anomaly into the ocean. **d.** Shortwave heat flux anomaly into the ocean. The data are from the GFDL ODA.
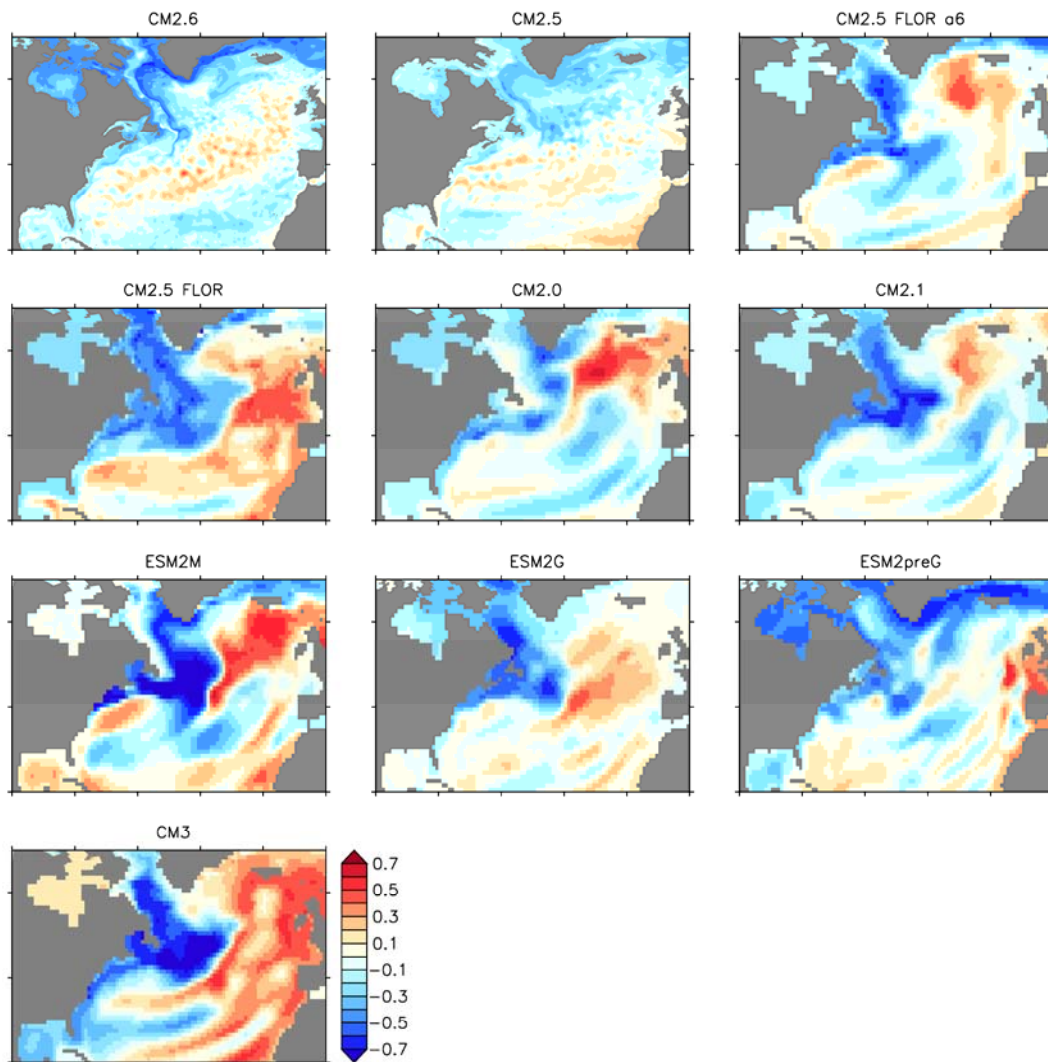
Supplementary Figure 7. Correlation between the annual mean DSL and AMOC data in the control runs of 10 GFDL models. All control runs are 100-year long except CM2.6 (80-year long). The AMOC index is defined as the maximum overturning streamfunction at 45°N in the North Atlantic.
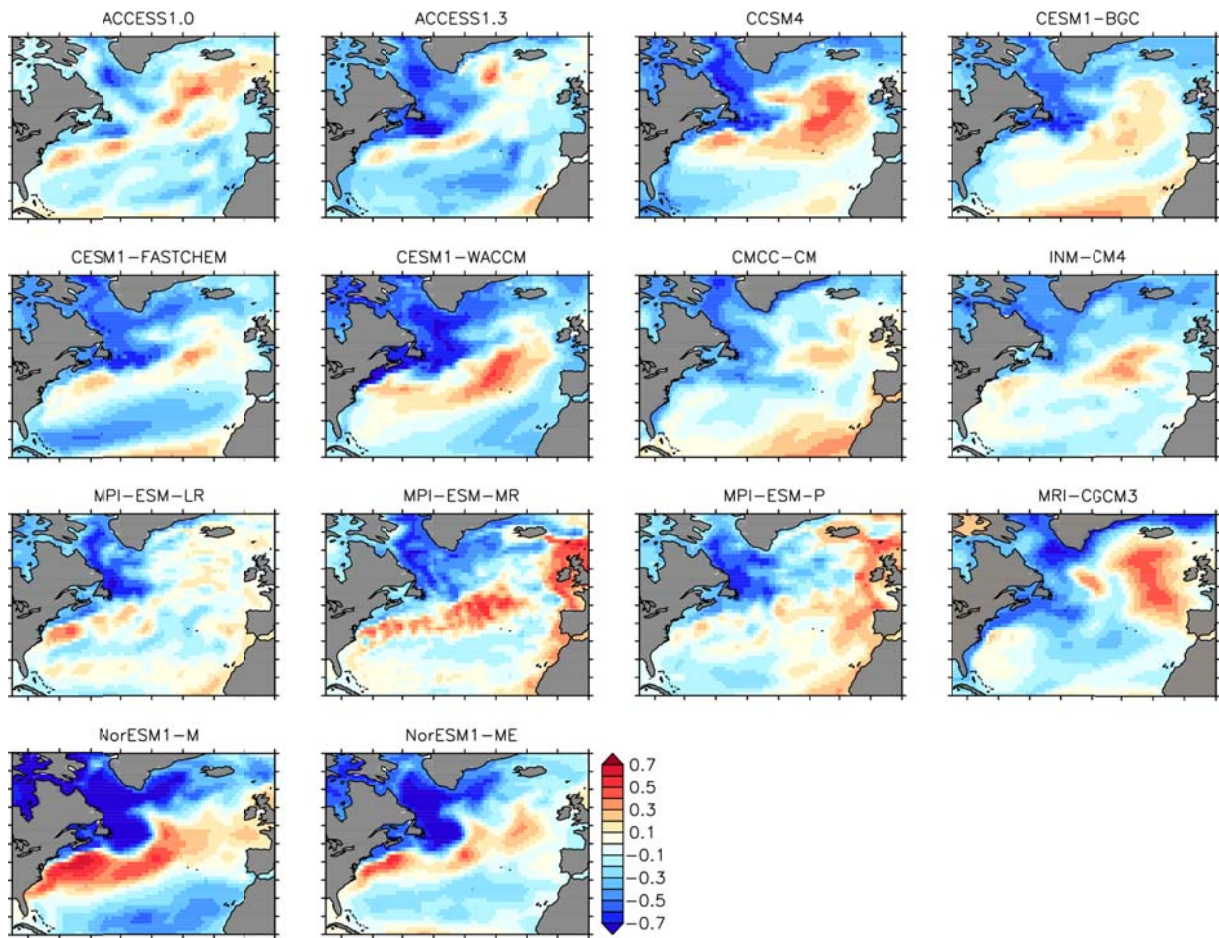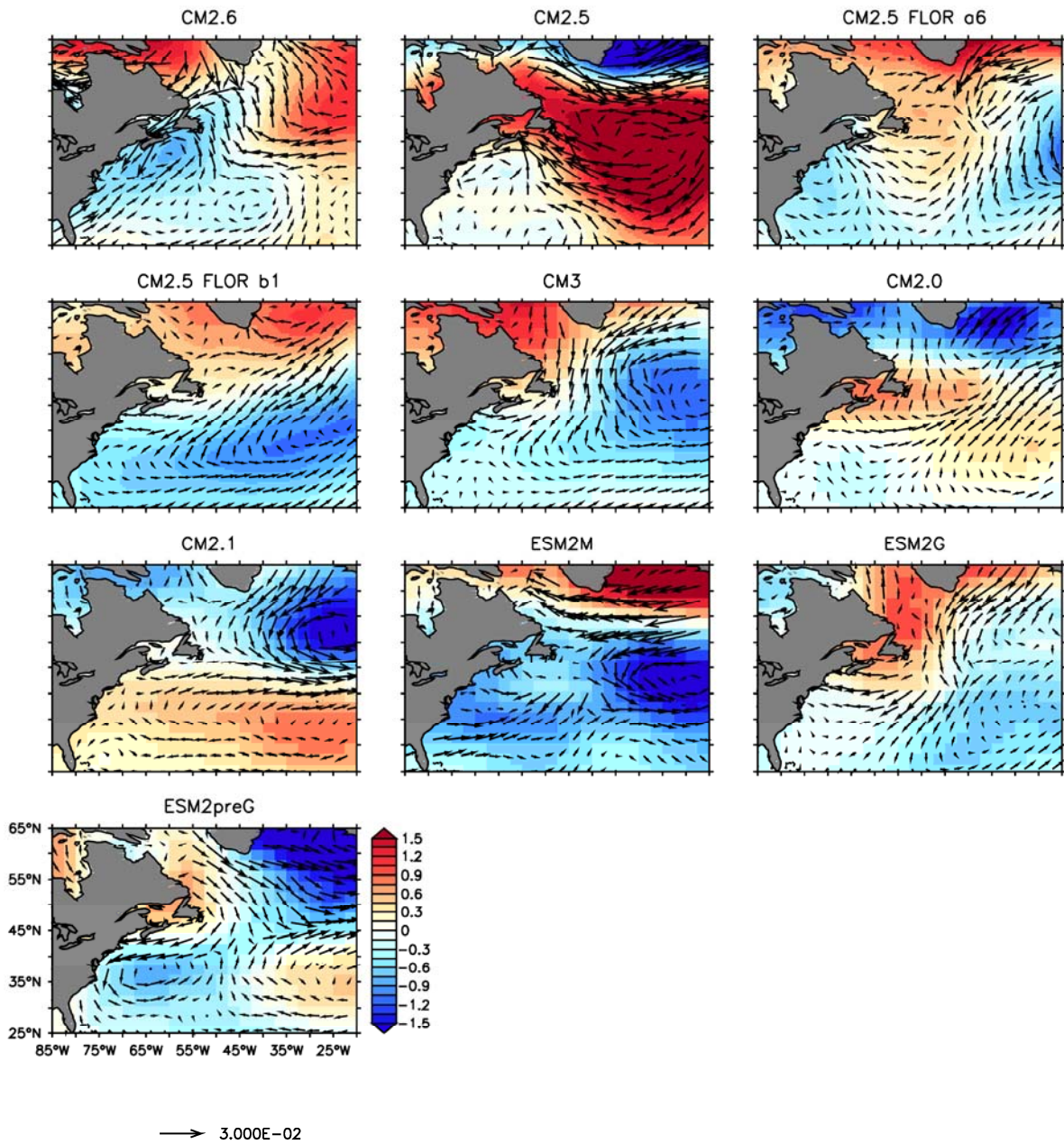
Supplementary Figure 8. Correlation between the annual mean DSL and AMOC data in the control runs of 14 CMIP5 models. All control runs are 100-year long.
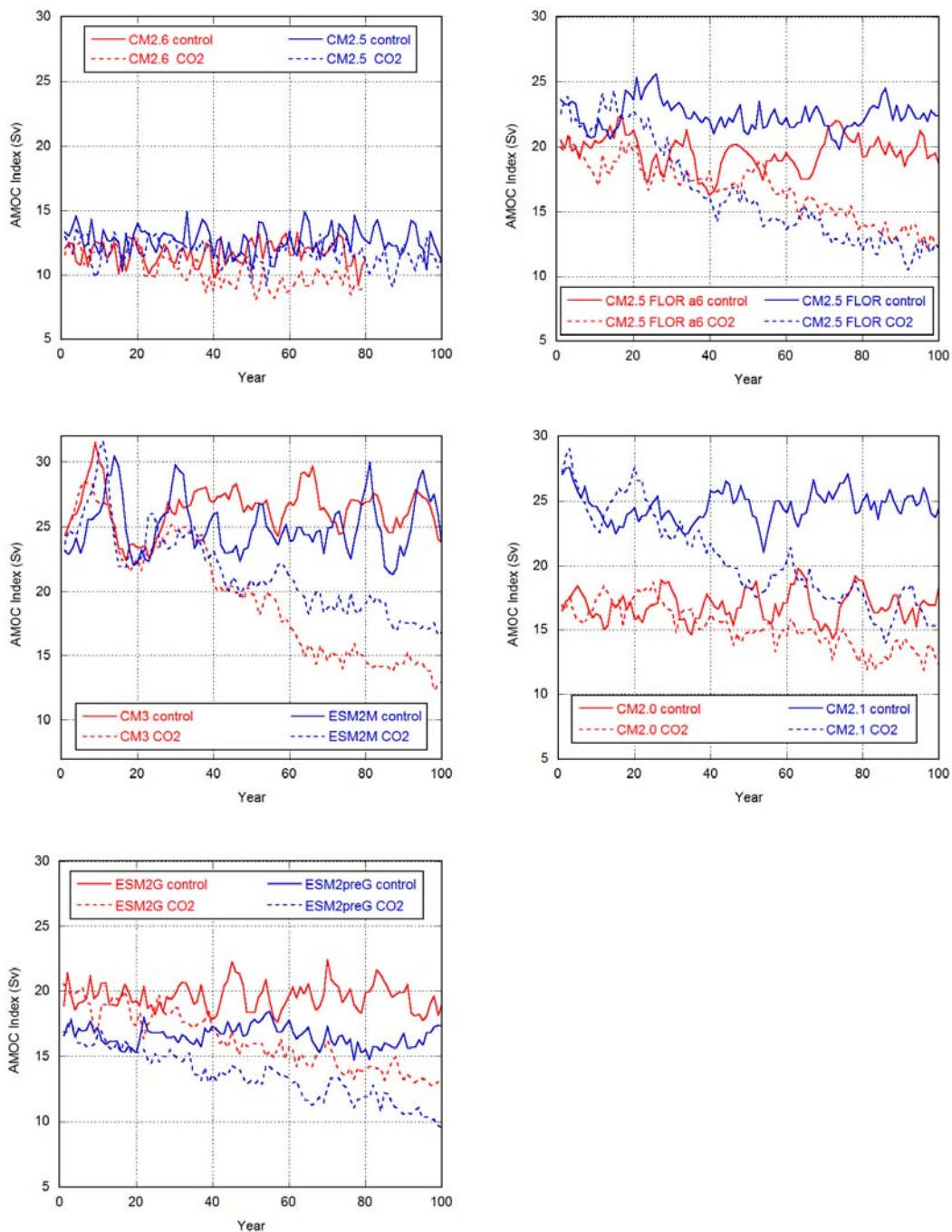
Supplementary Figure 9. Time series of the AMOC index (45°N) in the control runs and 1% yr^{-1} CO$_2$ experiments of the 10 GFDL models.

Supplementary Figure 10. Wind stress and sea level pressure anomaly patterns during coastal extreme SLR events in the control runs of 10 GFDL models. This figure shows the mean difference of sea level pressure (hPa) and wind stress (N m^{-2}) between the years in which the yearly SLR rates near Boston are greater than 20 mm yr^{-1} verse less than -20 mm yr^{-1}.
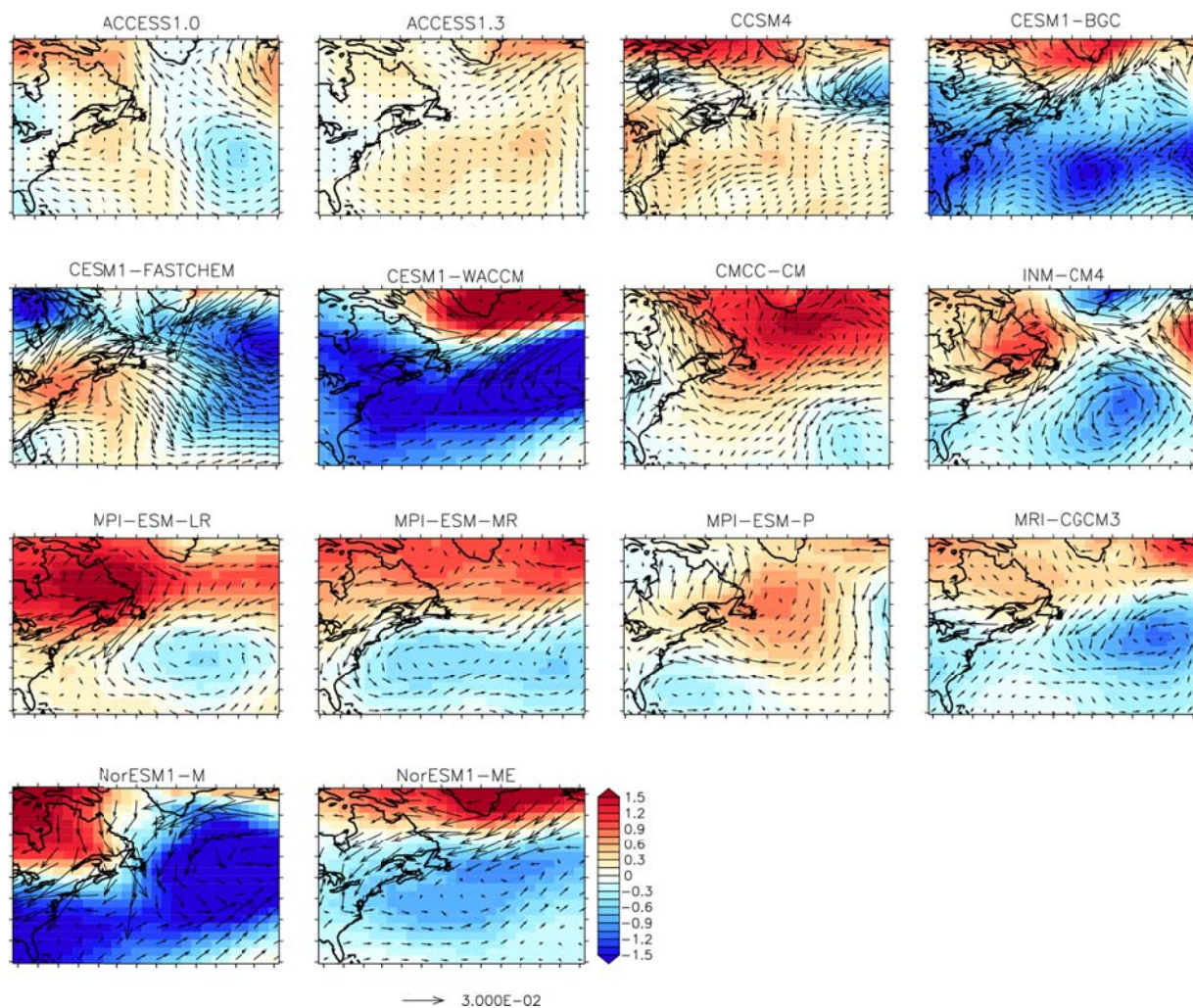
Supplementary Figure 11. Wind stress and sea level pressure anomaly patterns during coastal extreme SLR events in the control runs of 14 CMIP5 models. This figure shows the mean difference of sea level pressure (hPa) and wind stress (N m^{-2}) between the years in which the yearly SLR rates near Boston are greater than 20 mm yr^{-1} verse less than -20 mm yr^{-1}.
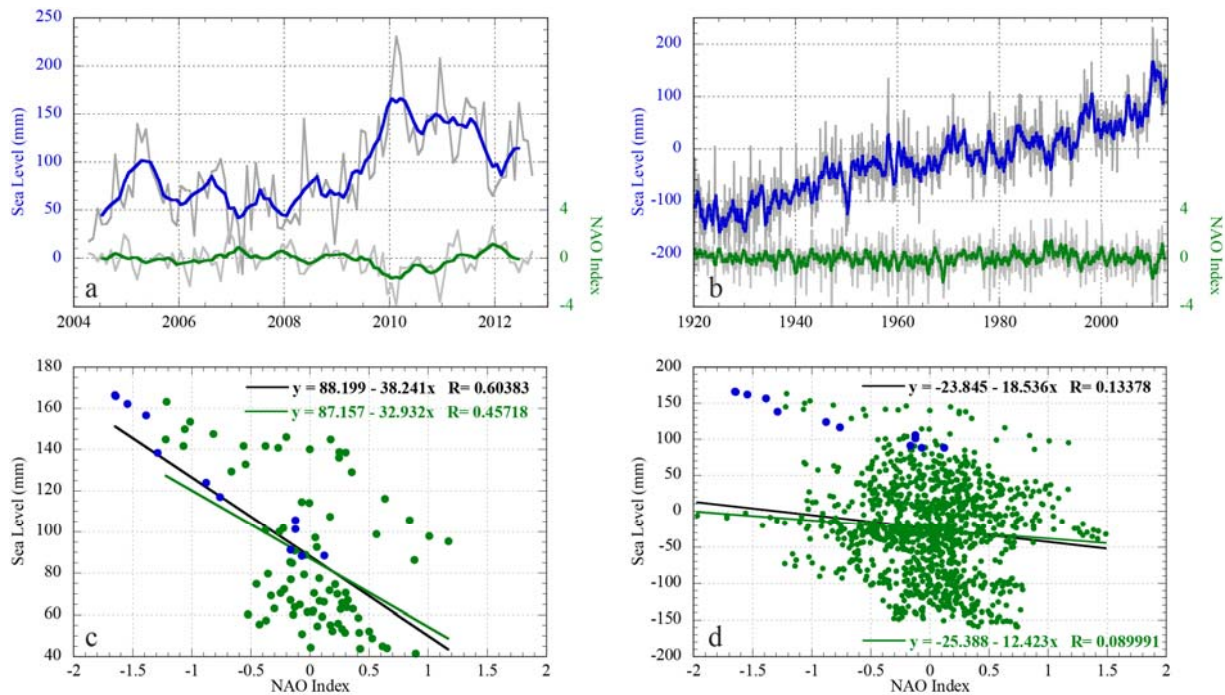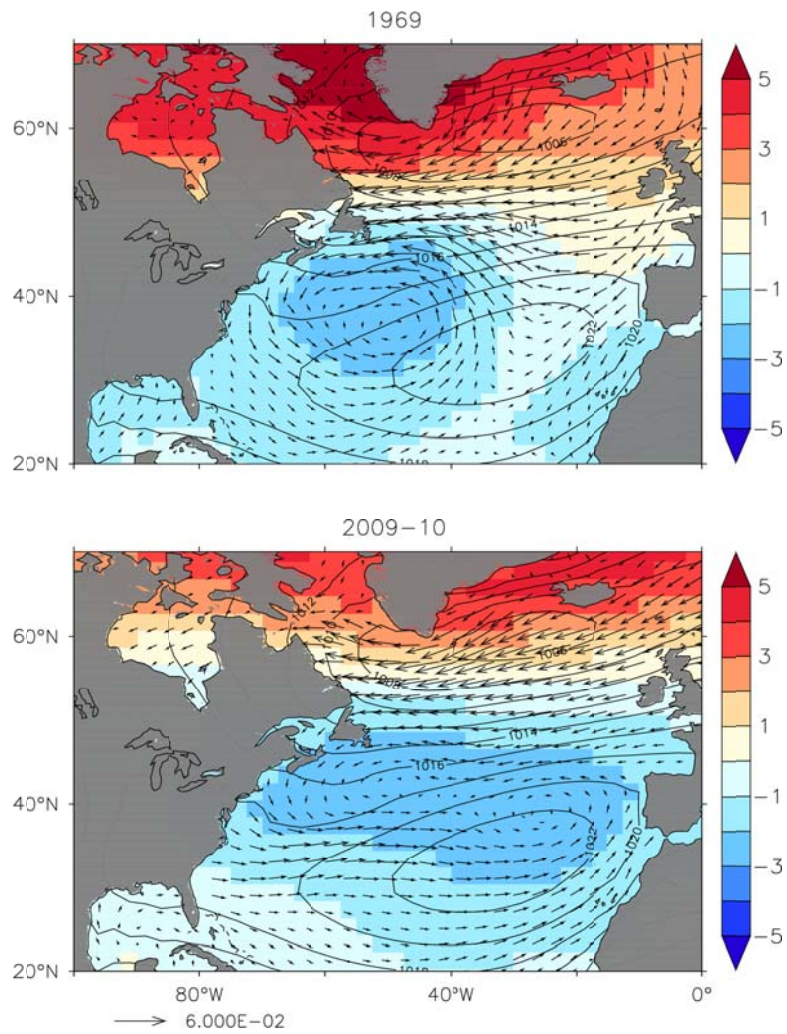
Supplementary Figure 12. Correlation between the NAO index and the Northeast sea level composite. a. The time series of the NE sea level composite (monthly gray, filtered blue) and the NAO index (monthly light gray, filtered green). The seasonal cycle has been removed from the NE composite and a 6-month filter applied to both time series. **b.** Same as **a.** but for a much longer time period (January 1920-September 2012). **c.** The monthly correlation and regression between the NAO index and NE sea level composite. The blue points highlight the correlation during the 30% AMOC downturn period. The green trend line is calculated from the green points only which are the months not associated with the 30% downtown period of the AMOC. The black trend line is calculated from all points (April 2004-September 2012). **d.** Same as **c.** but for a much longer time period (January 1920-September 2012). The sea level data are from PSMSL. The NAO index data are obtained from the NCAR Climate Analysis Section (https://climatedataguide.ucar.edu/climate-data/hurrell-north-atlantic-oscillation-nao-index-station-based).

Supplementary Figure 13. Two periods with extreme negative NAO index: 1969 and 2009-10. Shading and vectors show the sea level pressure anomalies (hPa) and the wind stress anomalies (N m^{-2}), respectively. Contours indicate sea level pressure climatology (hPa).
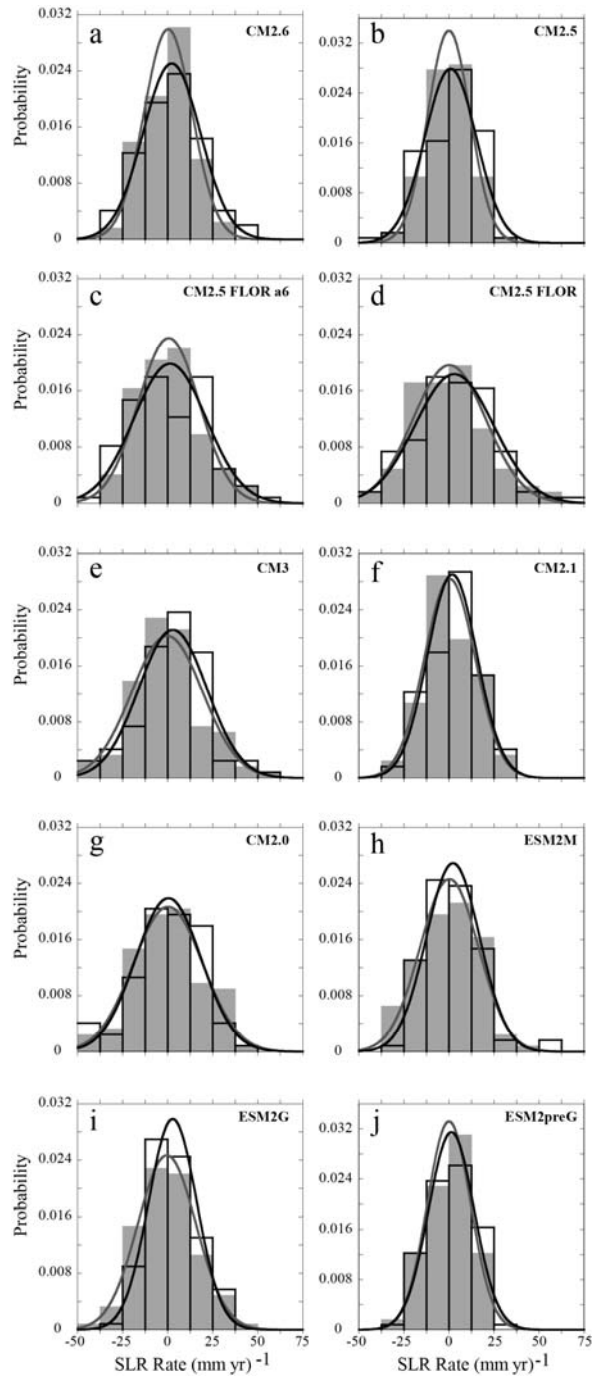
Supplementary Figure 14. Distribution of the yearly SLR rates in the simulations of the 10 GFDL models. The values show the composite SLR rates along the Northeast Coast of North America. The yearly SLR rates are calculated based on both the DSL changes and the global ocean thermal expansion. All runs are 100-year long except CM2.6 (80-year long). Shading and gray – control runs; thick black lines – CO_2 experiments. Fits are from Gaussian distribution.

Supplementary Table 1. TG data in three SLR regimes used in the present study.

Station Name	Latitude (°N)	Longitude (°W)	Record Span Used	Completeness
Key West	24.56	81.81	1920-2012	99%
Fernandia	30.67	81.47	1920-2012	77%
Fort Pulaski	32.03	80.90	1935-2012	97%
Charleston 1	32.78	79.93	1922-2012	100%
Springmaid Pier	33.66	78.92	1978-2012	71%
Wilmington	34.23	77.95	1936-2012	96%
Duck Pier Outside	36.18	75.75	1985-2011	93%
Sewells Point	36.95	76.33	1928-2012	100%
Chesapeake Bay	36.97	76.11	1985-2012	100%
Kiptopeke	37.17	75.99	1952-2012	97%
Solomon's Island	38.32	76.45	1938-2012	95%
Cambridge II	38.57	76.07	1971-2012	95%
Lewes	38.78	75.12	1920-2012	70%
Cape May	38.97	74.96	1966-2012	89%
Annapolis	38.98	76.48	1929-2012	94%
Baltimore	39.27	76.58	1920-2012	99%
Atlantic City	39.36	74.42	1920-2012	86%
Reedy Point	39.56	75.57	1985-2012	79%
Philadelphia Pier 9N	39.93	75.14	1920-2012	95%
Sandy Hook	40.47	74.01	1933-2011	96%
Bergen Point	40.64	74.14	1985-2012	79%
New York (Battery)	40.70	74.01	1920-2012	97%
Montauk	41.05	71.96	1948-2012	83%
Bridgeport	41.17	73.18	1965-2012	92%
Nantucket Island	41.29	70.10	1965-2012	92%
New London	41.36	72.09	1939-2012	93%
Newport	41.51	71.33	1931-2012	98%
Woods Hole	41.52	70.67	1933-2012	90%
Providence	41.81	71.40	1939-2012	82%
Boston	42.35	71.05	1921-2012	98%
Portland	43.66	70.25	1920-2012	99%
Yarmouth	43.83	66.13	1967-2012	71%
Bar Harbor	44.39	68.21	1948-2012	85%
Halifax	44.67	63.58	1920-2012	91%
Eastport	44.90	66.98	1930-2012	87%
North Sydney	46.22	60.25	1971-2012	88%
Charlottetown	46.23	63.12	1971-2011	88%
Argentia	47.30	53.98	1972-2012	70%
Port-Aux-Basques	47.57	59.13	1959-2010	77%
Rimouski	48.48	68.52	1985-2012	82%